



Providing Choice & Value

Generic CT and MRI Contrast Agents



**FRESENIUS
KABI**

CONTACT REP

AJNR

**White Matter Alterations in Spastic
Paraplegia Type 5: A Multiparametric
Structural MRI Study and Correlations with
Biochemical Measurements**

Y. Liu, Z. Ye, J. Hu, Z. Xiao, F. Zhang, X. Yang, W. Chen,
Y. Fu and D. Cao

This information is current as
of July 23, 2025.

AJNR Am J Neuroradiol published online 18 November
2021

<http://www.ajnr.org/content/early/2021/11/18/ajnr.A7344>

White Matter Alterations in Spastic Paraplegia Type 5: A Multiparametric Structural MRI Study and Correlations with Biochemical Measurements

Y. Liu, Z. Ye, J. Hu, Z. Xiao, F. Zhang, X. Yang, W. Chen, Y. Fu, and D. Cao



ABSTRACT

BACKGROUND AND PURPOSE: In spastic paraplegia type 5, spinal cord atrophy and white matter signal abnormalities in the brain are the main MR imaging alterations. However, the specific mechanism remains unclear. We explored the microstructural changes occurring in spastic paraplegia type 5 and assessed the relation between MR imaging and clinical data.

MATERIALS AND METHODS: Seventeen patients with spastic paraplegia type 5 and 17 healthy controls were scanned with DTI and T1 mapping on a 3T MR imaging scanner. Fractional anisotropy, mean diffusivity, radial diffusivity, axial diffusivity, and T1 values were obtained using Tract-Based Spatial Statistics and the Spinal Cord Toolbox. Neurofilament light and myelin basic protein in the CSF were measured. The differences in MR imaging and biochemical data between patients with spastic paraplegia type 5 and healthy controls were compared using the Student *t* test.

RESULTS: A widespread reduction of fractional anisotropy values and an elevation of mean diffusivity, T1, and radial diffusivity values were found in most cervical, T4, and T5 spinal cords; corona radiata; optic radiations; and internal capsules in spastic paraplegia type 5. A variation in axial diffusivity values was shown only in C2, C6, and the corona radiata but not in the gray matter. The levels of neurofilament light and myelin basic protein were higher in those with spastic paraplegia type 5 than in healthy controls (myelin basic protein, 3507 [SD, 2291] versus 127 [SD, 219] pg/mL; neurofilament light, 617 [SD, 207] versus 265 [SD, 187] pg/mL; $P < .001$). No correlation was found between the clinical data and MR imaging–derived measures.

CONCLUSIONS: Multiparametric MR imaging and biochemical indicators demonstrated that demyelination (mainly) and axonal loss led to the white matter integrity loss without gray matter injury in spastic paraplegia type 5.

ABBREVIATIONS: AD = axial diffusivity; FA = fractional anisotropy; HC = healthy control; HSP = hereditary spastic paraplegia; MBP = myelin basic protein; MD = mean diffusivity; NFL = neurofilament light; RD = radial diffusivity; SPG5 = spastic paraplegia type 5; SPRS = Spastic Paraplegia Rating Scale

Hereditary spastic paraplegia (HSP) is a neurodegenerative disorder characterized by retrograde axonal degeneration of the corticospinal tracts.¹ Spastic paraplegia type 5 (SPG5) is a rare subtype of HSP for which treatment with cholesterol-lowering

drugs can be attempted,² but the target of drug action remains uncertain. Recent evidence has indicated that SPG5 is caused by a recessive mutation in the oxysterol-7 α -hydroxylase gene *CYP7B1*, which leads to the accumulation of neurotoxic oxysterols, especially 27-hydroxycholesterol (27-OHC), which was found to impair the viability of human cortical neurons in SPG5.^{2–4} Given that axons in the white matter are known to exert essential functions in lipid transport,⁵ we hypothesized that patients with SPG5 might have white matter integrity loss. An improved understanding of white matter integrity loss patterns (ie, demyelination and/or dying-back axonopathy) would be of substantial clinical relevance for enabling personalized treatment approaches for patients with SPG5.^{6,7}

DTI is a robust method to detect in vivo white matter abnormalities. Specifically, radial diffusivity (RD) values can provide a quantitative evaluation of myelin sheaths, while axial diffusivity (AD) values support the assessment of axon status.^{8,9} Accordingly, DTI has been used to evaluate common subtypes of HSP, such as

Received July 16, 2021; accepted after revision September 10.

From the Departments of Radiology (Y.L., J.H., F.Z., X.Y., D.C.) and Neurology and Institute of Neurology (Z.Y., W.C., Y.F.), and Key Laboratory of Radiation Biology of Fujian Higher Education Institutions (D.C.), First Affiliated Hospital, Fujian Medical University, Fuzhou, China; Department of Medical Imaging Technology (Y.L.), College of Medical Technology and Engineering, Department of Neurology and Institute of Neurology (Z.Y., W.C., Y.F.), and Fujian Key Laboratory of Molecular Neurology (W.C.), Fujian Medical University, Fuzhou, China; and Department of Biomedical Sciences (Z.X.), University of Pennsylvania, Philadelphia, Pennsylvania.

Ying Liu and Zhixian Ye contributed equally to this study.

This work was supported by a Startup Fund for Scientific Research, Fujian Medical University (2017XQ1016).

Please address correspondence to Dairong Cao, MD, Department of Radiology of The First Affiliated Hospital of Fujian Medical University, No. 20, Chazhong Rd, Taijiang District, Fuzhou, Fujian, 350005, China; e-mail: dairongcao@163.com

Indicates article with online supplemental data.

<http://dx.doi.org/10.3174/ajnr.A7344>

SPG4 and SPG11.^{10–14} However, to date, no study has reported using DTI to assess both the brain and spinal cord of SPG5. One challenge with the application of DTI to HSPs is that physiologic motion and susceptibility artifacts in the spinal cord can challenge DTI quality. T1 mapping, which is relatively less susceptible to artifacts, can reflect myelin conditions and could potentially complement DTI to explore the myelin injury in HSP; the working principle of T1 mapping exploits the relatively faster relaxation of myelin water compared with nonmyelin water.¹⁵ Moreover, neurofilament light (NFL) and myelin basic protein (MBP) in the CSF are promising biomarkers that can accurately reflect neuroaxonal loss and myelin damage, respectively.^{16,17}

In this study, we performed multiparametric structural MR imaging, including DTI and T1 mapping, to investigate the brain and spinal cord microstructural alterations in 17 patients with genetically confirmed SPG5 and conducted biochemical measurements to verify observed trends in myelin and axonal damage. Subsequently, we explored the correlations of these indicators with clinical manifestations.

MATERIALS AND METHODS

Subject Selection

Participants were prospectively recruited into the registered cohort spastic paraplegia study (National Clinical Trials: 04006418) from 2019 to 2020. This case-control parallel cohort study received approval from the local ethical committees (The First Affiliated Hospital of Fujian Medical University). All the participants agreed to participate and signed an informed consent form.

Seventeen patients with SPG5 with genetic confirmation were included (Online Supplemental Data), and 17 age- and sex-matched healthy controls (HCs) were also recruited for imaging assessment. Eleven inpatients without neurologic diseases requiring a subarachnoid block in anesthesia served as controls for CSF biochemical evaluation (Online Supplemental Data).

Clinical and Biochemical Measurements

All participants completed neurologic examinations and CSF collection on the same day as the MR imaging examination. Disease severity was quantified with the Spastic Paraplegia Rating Scale (SPRS).¹⁸ CSF NFL was measured using Simoa NF-light Advantage Kits (Quanterix) on a Simoa HD-1 Analyzer instrument. MBP was measured by a Human MBP DuoSet ELISA (R&D Systems).

MR Imaging Acquisition

All participants underwent an examination on a 3T MR scanner (Magnetom Skyra; Siemens) equipped with a 20-channel head-neck coil and a 24-channel spine-array coil. The following sequences were performed: 1) axial T2WI, T2-FLAIR, and sagittal 3D T1WI covering the whole brain; 2) sagittal 3D-T2WI and 3D-T1WI covering the cervical and thoracic spinal cord; 3) DTI with a single-shot echo-planar imaging sequence for both brain and spinal cord (32 and 20 different gradient directions, respectively); and 4) a T1-mapping sequence based on B₁ inhomogeneity-corrected variable flip angle methods for the spinal cord. DTI and T1 mapping consisted of 2 axial slabs in the spinal cord: cervical (C2–C7) and thoracic (T1–T5) slabs. The parameters are listed in the Online Supplemental Data.

Image Processing

MR Imaging Analysis. DWI preprocessing was performed on the basis of FSL (<http://fsl.fmrib.ox.ac.uk/fsl>) and the Diffusion Toolkit (DTK; <http://www.trackvis.org/dtk/>). The 3D T1WIs were preprocessed using the CAT12 toolbox of Statistical Parametric Mapping, Version 12 (SPM; <http://www.fil.ion.ucl.ac.uk/spm/software/spm12>). Spinal cord images were analyzed on the basis of the open-source software Spinal Cord Toolbox (Version 4.01; <https://spinalcordtoolbox.com/>) (Online Supplemental Data).¹⁹

Brain Image Analysis. The DTI analysis of the brain was performed with Tract-Based Spatial Statistics (TBSS; <http://fsl.fmrib.ox.ac.uk/fsl/fslwiki/TBSS>). Voxel-based whole-brain white matter measures (DTI metrics) were assessed with TBSS using FSL 5.0 (<http://www.fmrib.ox.ac.uk/fsl>).

Voxel-based morphometry analysis was performed to analyze the alterations in the gray matter using the CAT12 toolbox.

Spinal Cord Image Analysis. Atlas-based analyses of spinal cord DTI and T1-mapping data were performed. The analysis pipeline is shown in the Online Supplemental Data. The spinal cord segments that met the quality control requirements are summarized in the Online Supplemental Data.

Statistical Analysis. Statistical analyses were performed with SPSS (Version 26; IBM). The sample size was determined by the number of eligible patients willing to participate without prospective calculation. Demographic, clinical, and biochemical variables were compared between SPG5 and HCs groups by means of Student *t* and Pearson χ^2 tests. Bonferroni adjustment was used to correct for multiple comparisons. Correlations were analyzed, counting age and sex as nuisance covariates.

TBSS statistical analysis was performed using a nonparametric permutation inference tool, FSL Randomize (<http://fsl.fmrib.ox.ac.uk/fsl/fslwiki/Randomise/UserGuide>). DTI metrics were compared between 2 groups using a 2-sample independent *t* test. A voxelwise 2-sample *t* test was conducted to detect the differences in the gray matter between patients with SPG5 and HCs. The total intracranial volume of each participant was entered as a covariate of no interest. Statistical inferences were made at $P < .001$ (uncorrected) and for clusters larger than $\kappa = 20$.

RESULTS

Demographic and Clinical Features

The demographic and clinical data of all participants are shown in the Table. According to the Harding criteria,²⁰ 16 patients had pure HSP and 1 patient had complicated HSP. All 17 patients presented with lower limb spasticity and weakness and dorsal column dysfunction. Sixteen patients had a severely reduced or non-existent vibration sense in the lower limbs.

The CSF MBP levels and CSF NFL levels in patients with SPG5 (CSF MBP, 3507 [SD, 2291] versus 127 [SD, 219] pg/mL, $P < .001$; CSF NFL, 617 [SD, 207] versus 265 [SD, 187] pg/mL; $P < .001$) were both higher than those in the control group. However, the increased degree in MBP was much higher than that in NFL in patients with SPG5 (compared with controls, the MBP increased by 27.61 [3507/127]

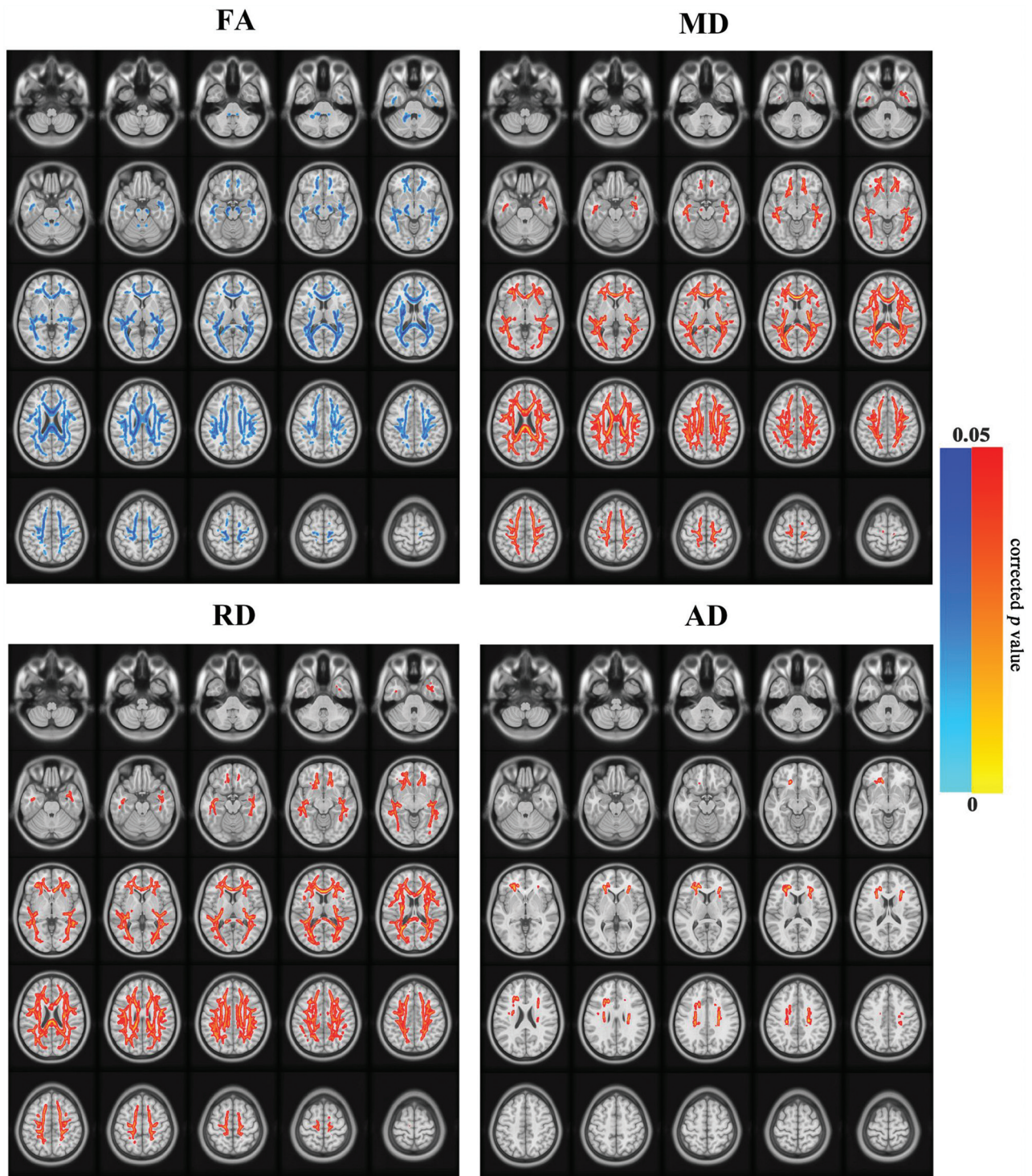


FIG 1. Images show whole-brain voxel-based analysis. Voxelwise FA, MD, RD, and AD comparisons by TBSS analysis.

folds on average, while the NFL increased only by 2.33 [617/265] in patients with SPG5). Conventional MR imaging showed no apparent signal abnormalities in the brain or spinal cord of those with SPG5 or HCs.

Brain MR Imaging Analysis

TBSS Analysis. Compared with HCs, an extensive and bilateral symmetric reduction of fractional anisotropy (FA) and an

elevation of mean diffusivity (MD) and RD were found in the cerebral peduncles, optic radiation, internal capsules, corona radiata, corpus callosum, posterior thalamic radiation, cingulum, and superior and inferior longitudinal fasciculi of patients with SPG5. The areas of elevated RD and MD closely mirrored the areas featuring reduced FA. However, an elevation of AD reached a statistically significant level only in the corona radiata (Fig 1).

Demographic and clinical data of study participants^a

Characteristic	HC ¹	HC ²	SPG5	P Value ¹	P Value ²
Participants ^b	17	11	17	>.99 ^c	<.01 ^c
Sex ^b				.99 ^c	.98 ^c
Men	11	8	11		
Women	6	3	6		
Age (yr) ^e	29 (SD, 10) (14–49)	39 (SD, 18) (11–69)	30 (SD, 10) (13–49)	.93 ^d	.13 ^d
SPRS ^e			16 (SD, 9) (2–38)		
Disease duration (yr) ^e			18 (SD, 10) (6–37)		

^a1 = Healthy controls recruited for imaging assessment, 2 = hospitalized patients requiring subarachnoid block in anesthesia without neurologic disease enrolled as controls for CSF biochemical assessment.

^bData are numbers of participants.

^cPearson χ^2 test.

^dStudent *t* test.

^eData are mean (SD). Data in parentheses are ranges.

Voxel-Based Morphometry Analysis. There were no statistically significant differences in gray matter volume between patients with SPG5 and HCs with a less conservative threshold ($P < .001$, uncorrected).

Spinal Cord Analysis. Compared with HCs, patients with SPG5 had reduced FA values and elevated RD, MD, and T1 values at the C2–T5 segments in the white matter, dorsal columns, and bilateral lateral corticospinal tract. Significant differences of FA, RD, and T1 values in the white matter regions between patients with SPG5 and HCs were observed in most cervical spinal cords but not in the thoracic segments, except T4 and T5. In contrast, no evident differences of AD values were observed in most spinal cord segments, and marked reduced AD values were found only at specific segments (eg, C2 and C6) (Fig 2 and Online Supplemental Data). Notably, no significant differences in DTI metrics or T1 values were detected in spinal cord gray matter between patients with SPG5 and HCs (Online Supplemental Data).

Correlation Analysis. No correlations were found between DTI parameters and disease severity (SPRS scores) or disease duration using TBSS. DTI or T1 values at all spinal cord segments in patients with SPG5 did not correlate with the clinical data ($P > .05$, after adjustment for multiple comparisons).

DISCUSSION

This prospective study investigated microstructural alterations occurring in patients with SPG5. First, the FA values of the brain and spinal cord white matter were reduced diffusely, indicative of widespread white matter injury in SPG5. Second, the RD, AD, T1 values, and biochemical indicators (NFL and MBP) demonstrated that the white matter injury pattern of SPG5 was demyelination (mainly). Third, there were no correlations between the degree of white matter injury and the clinical data in SPG5.

Although case reports showed scattered high signal intensity in the cerebral white matter,^{21,22} our patients with SPG5 demonstrated a normal appearance on conventional MR imaging (16 of 17 were pure HSP), like the “pure” phenotype HSP that has been reported without white matter abnormalities.^{23,24} However, reduced FA in the brain and spinal cord revealed white matter integrity loss in patients with SPG5. Meanwhile, corticospinal tract and dorsal column involvement was consistent with the clinical

symptoms: lower limb spasticity, weakness, and dorsal column dysfunction. In addition, we noted that the optic radiations were also affected in SPG5, though there were no clinical manifestations. Therefore, SPG5-specific widespread white matter defects were possibly related to the accumulation of 27-OHC²² rather than a genetic cause of damage to a specific site. On the basis of MR imaging, we have demonstrated the clinical feasibility of treating patients with SPG5 by lowering the pathologically elevated levels of oxysterols.²⁵

Reduced FA could be caused by axonal loss and/or myelin breakdown. RD and AD values derived from DTI can, respectively, indicate myelin sheath and axon status.²⁶ Our findings showed that RD increased in both the spinal cord and brain; AD values varied in only several cervical spinal cord segments and brain regions. These findings suggest that the white matter damage in SPG5 was more related to myelin destruction than to axonal loss. Similar to our results, an MR spectroscopy study showed an elevated mIns/Cr ratio in the occipitoparietal region in 2 patients, also indicating demyelination in SPG5.²⁷ Moreover, considering the limited stability of spinal cord DTI, we used the T1-mapping sequence to detect the possible myelin injury.²⁸ A prolonged T1-relaxation time in the spinal cord may indicate demyelination changes in SPG5 to some extent.

Furthermore, the NFL and MBP levels in the CSF were also analyzed to explore the myelin and axonal degeneration in SPG5. NFL is a component of the cytoskeleton of myelinated axons and can reflect axonal injury,¹⁶ while the MBP holds the layers of myelin together, so quantifying MBP supports the assessment of myelin destruction.¹⁷ Significant differences of both NFL and MBP were found between HCs and those with SPG5. Additionally, the mean MBP level in the CSF (3507 pg/mL) in our study was much higher than that in neuromyelitis optica (706 pg/mL) or multiple sclerosis (106 pg/mL);²⁹ the mean NFL level (617 pg/mL) was lower than that in Guillain-Barré syndrome (1308 pg/mL)³⁰ or multiple sclerosis (884 pg/mL).³¹

Thus, our DTI evidence and biochemical measurements together support the cautious deduction that the copresence of demyelination (mainly) and axonal loss resulted in white matter degeneration in SPG5. On the other hand, no gray matter abnormalities were found in the brain or spinal cord, in good agreement with the results of a previous MR spectroscopy study: no increased or reduced Cho/Cr ratio in the gray matter of the occipital

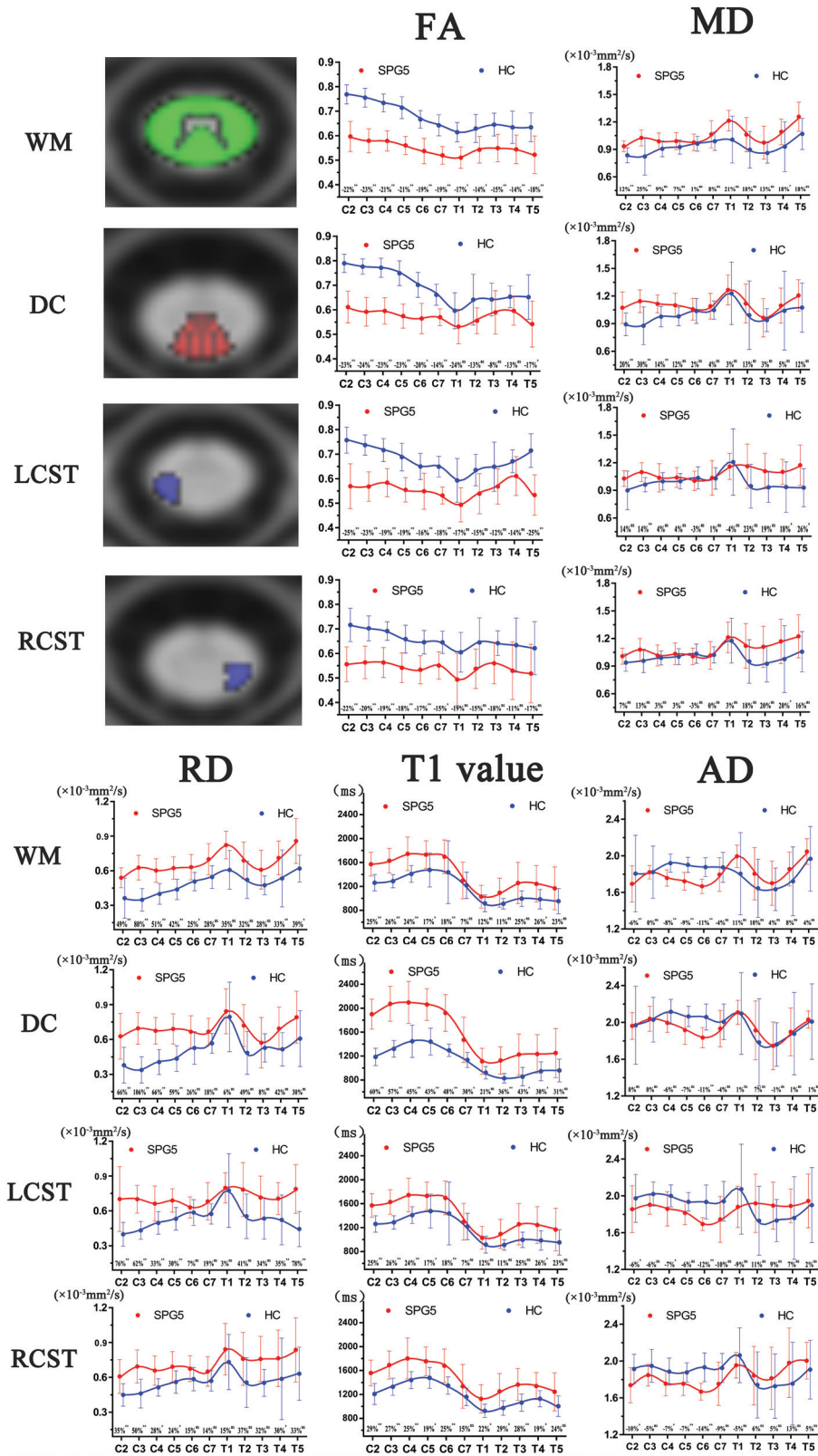


FIG 2. Analysis of DTI metrics and T1 values in 4 spinal cord regions. Percentage rates were calculated as follows: $(FA_{SPG5} - FA_{HC}) / FA_{HC}$. DC indicates dorsal column; LCST, left lateral corticospinal tract; RCST, right lateral corticospinal tract; WM, white matter.

region.²⁷ In brief, demyelination in both white matter and preserved gray matter in patients with SPG5 was consistent with the characteristics of pure HSP as reported in the literature^{12,14,32}

We found no correlations between clinical data (disease duration or SPRS scores) and MR imaging metrics. As previously reported,¹¹ the ceiling effect may be a good explanation. Patients

with SPG5 in our study were disabled and had a long disease duration (the mean SPRS of our patients was 16, the mean disease duration was 18 years); even though neurodegeneration was still taking place, the correlation analyses failed to capture clinical deterioration.³³ Meanwhile, considering the slowly progressive nature of the disease, white matter injury may be compensated by neuroaxonal redundancy or adaptive neuroplasticity, which led to a discrepancy between the functional evaluation of SPG5 patients and DTI structural assessment in SPG5.³⁴ Additionally, cholesterol is a vital component of myelin; we assumed that abnormalities in cholesterol metabolism could influence the early development of myelin before the degeneration.

Our study had several limitations. First, the interpretations of AD, RD, and T1 values are still contested.³⁵ Diffusional kurtosis imaging and neurite orientation dispersion and density imaging may be the optimal MR imaging techniques to strengthen the findings of this study.³⁵ Second, lumbar puncture is an invasive examination; the HCs who underwent the MR imaging examinations were not the same ones who underwent the lumbar puncture to get the biochemical measurements. Third, the data reliability of thoracic spinal cord DTI may be a problem in this study, which is expected to be solved by more sequence improvement.

CONCLUSIONS

Multiparametric structural MR imaging and biochemical measurements revealed that the neurodegeneration progression of SPG5 was related to white matter integrity loss (demyelination mainly) rather than neuronopathy. Our identification of the widespread myelin damage can support the development of SPG5 treatment regimens in the future.

ACKNOWLEDGMENTS

We thank all patients with SPG5 and healthy controls participating in this study.

Disclosure forms provided by the authors are available with the full text and PDF of this article at www.ajnr.org.

REFERENCES

- Salinas S, Proukakis C, Crosby A, et al. **Hereditary spastic paraplegia: clinical features and pathogenetic mechanisms.** *Lancet Neurol* 2008;7:1127–38 [CrossRef Medline](#)
- Schols L, Rattay TW, Martus P, et al. **Hereditary spastic paraplegia type 5: natural history, biomarkers and a randomized controlled trial.** *Brain* 2017;140:3112–27 [CrossRef Medline](#)
- Schule R, Wiethoff S, Martus P, et al. **Hereditary spastic paraplegia: clinicogenetic lessons from 608 patients.** *Ann Neurol* 2016;79:646–58 [CrossRef Medline](#)
- Bjorkhem I, Leoni V, Meaney S. **Genetic connections between neurological disorders and cholesterol metabolism.** *J Lipid Res* 2010;51:2489–503 [CrossRef Medline](#)
- Vance JE, Campenot RB, Vance DE. **The synthesis and transport of lipids for axonal growth and nerve regeneration.** *Biochim Biophys Acta* 2000;1486:84–96 [CrossRef Medline](#)
- Tsaousidou MK, Ouahchi K, Warner TT, et al. **Sequence alterations within CYP7B1 implicate defective cholesterol homeostasis in motor-neuron degeneration.** *Am J Hum Genet* 2008;82:510–15 [CrossRef Medline](#)
- Criscuolo C, Filla A, Coppola G, et al. **Two novel CYP7B1 mutations in Italian families with SPG5: a clinical and genetic study.** *J Neurol* 2009;256:1252–57 [CrossRef Medline](#)
- Alexander AL, Lee JE, Lazar M, et al. **Diffusion tensor imaging of the brain.** *Neurotherapeutics* 2007;4:316–29 [CrossRef Medline](#)
- Qiu D, Tan LH, Zhou K, et al. **Diffusion tensor imaging of normal white matter maturation from late childhood to young adulthood: voxel-wise evaluation of mean diffusivity, fractional anisotropy, radial and axial diffusivities, and correlation with reading development.** *Neuroimage* 2008;41:223–32 [CrossRef Medline](#)
- Pan MK, Huang SC, Lo YC, et al. **Microstructural integrity of cerebral fiber tracts in hereditary spastic paraparesis with SPG11 mutation.** *AJNR Am J Neuroradiol* 2013;34:990–96 [CrossRef](#)
- Agosta F, Scarlato M, Spinelli EG, et al. **Hereditary spastic paraplegia: beyond clinical phenotypes toward a unified pattern of central nervous system damage.** *Radiology* 2015;276:207–18 [CrossRef Medline](#)
- Rezende TJ, de Albuquerque M, Lamas GM, et al. **Multimodal MRI-based study in patients with SPG4 mutations.** *PLoS One* 2015;10:e0117666 [CrossRef Medline](#)
- Oğuz KK, Sanverdi E, Has A, et al. **Tract-based spatial statistics of diffusion tensor imaging in hereditary spastic paraplegia with thin corpus callosum reveals widespread white matter changes.** *Diagn Interv Radiol* 2013;19:181–86 [CrossRef Medline](#)
- Lindig T, Bender B, Hauser TK, et al. **Gray and white matter alterations in hereditary spastic paraplegia type SPG4 and clinical correlations.** *J Neurol* 2015;262:1961–71 [CrossRef Medline](#)
- Battiston M, Schneider T, Prados F, et al. **Fast and reproducible in vivo T1 mapping of the human cervical spinal cord.** *Magn Reson Med* 2018;79:2142–48 [CrossRef Medline](#)
- Khalil M, Teunissen CE, Otto M, et al. **Neurofilaments as biomarkers in neurological disorders.** *Nat Rev Neurol* 2018;14:577–89 [CrossRef Medline](#)
- Lillico R, Zhou T, Khorshid Ahmad T, et al. **Increased post-translational lysine acetylation of myelin basic protein is associated with peak neurological disability in a mouse experimental autoimmune encephalomyelitis model of multiple sclerosis.** *J Proteome Res* 2018;17:55–62 [CrossRef Medline](#)
- Schule R, Holland-Letz T, Klimpe S, et al. **The Spastic Paraplegia Rating Scale (SPRS): a reliable and valid measure of disease severity.** *Neurology* 2006;67:430–34 [CrossRef Medline](#)
- De Leener B, Levy S, Dupont SM, et al. **SCT: Spinal Cord Toolbox, an open-source software for processing spinal cord MRI data.** *Neuroimage* 2017;145:24–43 [CrossRef Medline](#)
- Harding AE. **Classification of the hereditary ataxias and paraplegias.** *Lancet* 1983;1:1151–55 [CrossRef Medline](#)
- Biancheri R, Ciccolella M, Rossi A, et al. **White matter lesions in spastic paraplegia with mutations in SPG5/CYP7B1.** *Neuromuscul Disord* 2009;19:62–65 [CrossRef Medline](#)
- Chou CT, Soong BW, Lin KP, et al. **Clinical characteristics of Taiwanese patients with hereditary spastic paraplegia type 5.** *Ann Clin Transl Neurol* 2020;7:486–96 [CrossRef Medline](#)
- Dong EL, Wang C, Wu S, et al. **Clinical spectrum and genetic landscape for hereditary spastic paraplegias in China.** *Mol Neurodegener* 2018;13:36 [CrossRef Medline](#)
- Duning T, Warnecke T, Schirmacher A, et al. **Specific pattern of early white-matter changes in pure hereditary spastic paraplegia.** *Mov Disord* 2010;25:1986–92 [CrossRef Medline](#)
- Mignarri A, Malandrini A, Del Puppo M, et al. **Treatment of SPG5 with cholesterol-lowering drugs.** *J Neurol* 2015;262:2783–85 [CrossRef Medline](#)
- Noguerol TM, Barousse R, Amrhein TJ, et al. **Optimizing diffusion-tensor imaging acquisition for spinal cord assessment: physical basis and technical adjustments.** *Radiographics* 2020;40:403–27 [CrossRef Medline](#)
- Roos P, Svenstrup K, Danielsen ER, et al. **CYP7B1: novel mutations and magnetic resonance spectroscopy abnormalities in hereditary spastic paraplegia type 5A.** *Acta Neurol Scand* 2014;129:330–34 [CrossRef Medline](#)

28. Hofer S, Wang X, Roeloffs V, et al. **Single-shot T1 mapping of the corpus callosum: a rapid characterization of fiber bundle anatomy.** *Front Neuroanat* 2015;9:57 [CrossRef Medline](#)
29. Takano R, Misu T, Takahashi T, et al. **Astrocytic damage is far more severe than demyelination in NMO: a clinical CSF biomarker study.** *Neurology* 2010;75:208–16 [CrossRef Medline](#)
30. Martin-Aguilar L, Camps-Renom P, Lleixa C, et al. **Serum neurofilament light chain predicts long-term prognosis in Guillain-Barre syndrome patients.** *J Neurol Neurosurg Psychiatry* 2021;92:70–77 [CrossRef Medline](#)
31. Sejbaek T, Nielsen HH, Penner N, et al. **Dimethyl fumarate decreases neurofilament light chain in CSF and blood of treatment naive relapsing MS patients.** *J Neurol Neurosurg Psychiatry* 2019;90: jnnp-2019-321321–30 [CrossRef Medline](#)
32. Aghakhanyan G, Martinuzzi A, Frijia F, et al. **Brain white matter involvement in hereditary spastic paraplegias: analysis with multiple diffusion tensor indices.** *AJNR Am J Neuroradiol* 2014;35:1533–38 [CrossRef Medline](#)
33. Servelhere KR, Casseb RF, de Lima FD, et al. **Spinal cord gray and white matter damage in different hereditary spastic paraplegia subtypes.** *AJNR Am J Neuroradiol* 2021;42:610–15 [CrossRef Medline](#)
34. Castellano A, Papinutto N, Cadioli M, et al. **Quantitative MRI of the spinal cord and brain in adrenomyeloneuropathy: in vivo assessment of structural changes.** *Brain* 2016;139:1735–46 [CrossRef Medline](#)
35. Andica C, Kamagata K, Hatano T, et al. **MR biomarkers of degenerative brain disorders derived from diffusion imaging.** *J Magn Reson Imaging* 2020;52:1620–36 [CrossRef Medline](#)